

Thomas–Fermi–Dirac–von Weizsäcker models in finite systems

Garnet Kin-Lic Chan, Aron J. Cohen, and Nicholas C. Handy

Citation: **114**, (2001); doi: 10.1063/1.1321308

View online: <http://dx.doi.org/10.1063/1.1321308>

View Table of Contents: <http://aip.scitation.org/toc/jcp/114/2>

Published by the [American Institute of Physics](#)

Thomas–Fermi–Dirac–von Weizsäcker models in finite systems

Garnet Kin-Lic Chan,^{a)} Aron J. Cohen, and Nicholas C. Handy
Department of Chemistry, Lensfield Road, Cambridge CB2 1EW, United Kingdom

(Received 7 June 2000; accepted 8 September 2000)

To gain an understanding of the variational behavior of kinetic energy functionals, we perform a numerical study of the Thomas–Fermi–Dirac–von Weizsäcker theory in finite systems. A general purpose Gaussian-based code is constructed to perform energy and geometry optimizations on polyatomic systems to high accuracy. We carry out benchmark studies on atomic and diatomic systems. Our results indicate that the Thomas–Fermi–Dirac–von Weizsäcker theory can give an approximate description of matter, with atomic energies, binding energies, and bond lengths of the correct order of magnitude, though not to the accuracy required of a qualitative chemical theory. We discuss the implications for the development of new kinetic functionals. © 2001 American Institute of Physics. [DOI: 10.1063/1.1321308]

I. INTRODUCTION

Thomas–Fermi and related theories,^{1,2} where the Kohn–Sham kinetic energy $T_s[\rho] = \min_{\Psi_D \rightarrow \rho} \langle \Psi_D | \sum_i -1/2 \nabla_i^2 | \Psi_D \rangle$ is approximated by an explicit functional of the density, have been studied for many years and are the origin of modern density functional theory.^{3,4} An important advantage of such theories over the Kohn–Sham formulation is their simplicity, as they circumvent the need to solve the N coupled Kohn–Sham equations. Instead, the minimizing energy and density are yielded through the solution of the Euler equation,

$$\frac{\delta}{\delta \rho} [E - \mu N] = 0, \quad (1)$$

where normalization is enforced through the chemical potential μ , and ρ is constrained to be N representable.

Despite the efforts by many workers,^{5–14} it is still not clear to what extent and accuracy we can devise explicit density approximations to $T_s[\rho]$, especially in finite systems. We have recently shown¹⁴ that very accurate kinetic energies of molecules can be reproduced by a modification of Thomas–Fermi theory, when Hartree–Fock densities are supplied. This, however, does not guarantee a good variational performance in the Euler equation (1).

Further progress requires an understanding of the variational characteristics of Thomas–Fermi-type functionals. These must at least be gradient functionals (that is of the form $\int f(\rho, |\nabla \rho|) d\mathbf{r}$) as an extension of the Teller nonbinding theorem^{9,15–18} tells us that functionals without gradient corrections will not yield bound molecules. A suitable model to study is provided by the simplest gradient functional, the Thomas–Fermi–Dirac–von Weizsäcker functional. This is constructed as the sum of the Thomas–Fermi kinetic functional for the uniform electron gas,^{1,2}

$$T_s[\rho] = \frac{3}{10} (3\pi^2)^{2/3} \int \rho^{5/3} d\mathbf{r}, \quad (2)$$

the von Weizsäcker gradient correction¹⁹

$$T_w[\rho] = \frac{\lambda}{8} \int \frac{|\nabla \rho|^2}{\rho} d\mathbf{r}, \quad (3)$$

where λ is an adjustable parameter, the Dirac exchange functional,²⁰

$$E_x[\rho] = -\frac{3}{4} \left(\frac{3}{\pi} \right)^{1/3} \int \rho^{4/3} d\mathbf{r}, \quad (4)$$

and the usual Coulomb $1/2 \iint \rho(\mathbf{r}_1) \rho(\mathbf{r}_2) r_{12}^{-1} d\mathbf{r}_1 d\mathbf{r}_2$ and nuclear attraction $\int \rho v_{\text{ext}} d\mathbf{r}$ terms. Throughout this paper, we have used atomic units where $\hbar, m_e, |e|, 4\pi\epsilon_0 = 1$. We shall denote the above energy functional by TFD λ W; the neglect of the von Weizsäcker and exchange corrections leads to the TFD and TF functionals, respectively. While we have not studied spin effects in this work, the above formulas may be trivially modified to spin-density functional form by summation over α and β spin components.

As we have argued, an understanding of the variational characteristics of TFD λ W theory is important to the further development of Thomas–Fermi-type theories. However, due to numerical difficulties in solving the Euler equation (1),¹⁷ there is a lack of accurate numerical TFD λ W calculations in finite systems. We have not been able to find any numerical results performed to the level of accuracy one requires in a modern quantum chemical calculation, and with existing calculations^{6,9,11} disagreeing over the presence of binding in even diatomic molecules, we do not feel that a good understanding of TFD λ W theory is yet available.

For this reason, we have decided to undertake a numerical study of the TFD λ W model functionals in atomic and molecular systems. Using benchmark calculations, we aim to answer the fundamental questions of TFD λ W and related Thomas–Fermi-type models, such as the strength and qualitative properties of binding in molecules, and also to illustrate well-known results for the qualitative behavior of the density and chemical potential in a numerical manner.

The structure of our study is as follows. In Sec. II, we first establish the necessary background and recall some im-

^{a)}Electronic mail: gkc1000@hermes.cam.ac.uk

portant results in the study of the Thomas–Fermi-type model functionals. The qualitative influence of the von Weizsäcker term is discussed.

In Sec. III, we proceed to describe a practical method to solve the Euler equation (1). We introduce a Gaussian basis set to expand an orbital ϕ , with the density constructed as ϕ^2 , and our implementation can carry out energy evaluations and geometry optimizations on polyatomic systems in a similar manner to conventional quantum chemical calculations.

In Sec. IV, we perform numerical studies of atomic and diatomic systems. In our studies on atoms, we perform benchmark-level calculations on total energies. We also examine chemical potentials, ionization potentials, and densities of the atoms. In our studies on diatomics, we perform benchmark-level calculations to definitively address the problem of binding. We present binding curves, binding energies, and bond distances for a variety of first row diatomics. We also examine the role of the λ parameter of the TFD λ W model in determining the equilibrium geometry and binding energy.

Finally, in Sec. V, we draw our conclusions, and discuss our results in the wider context of the future development of kinetic energy functionals for finite systems.

II. PROPERTIES OF THOMAS–FERMI-TYPE MODELS IN FINITE SYSTEMS

In this section, we present some background theory, as well as a few new remarks on Thomas–Fermi-type models in finite systems. Further background theory may be found in various texts.^{17,21}

We begin with TF theory. In neutral atoms, which have $\mu=0$, the TF energy is given by the formula¹⁷

$$E = -0.7687Z^{7/3}. \quad (5)$$

The TF density diverges at the nucleus like $r^{-3/2}$, and far away decays like r^{-6} .¹⁷ These qualitative features are not improved in TFD theory, where neutral atoms have finite size. Furthermore, in TF theory, anions are unbound, and cations have a finite size. However, TF theory is exact in the limit as $Z \rightarrow \infty$, as has been demonstrated by Lieb and Simon.⁷ By this, we mean that the exact density ρ_0 and energy E_0 , and Thomas–Fermi density ρ , and energy E , for a set of nuclear charges Z_α and positions R_α are related by

$$\lim_{\lambda \rightarrow \infty} \lambda^{-7/3} E_0(\lambda Z_\alpha, \lambda N, \lambda R_\alpha) = \lim_{\lambda \rightarrow \infty} \lambda^{-7/3} E(\lambda Z_\alpha, \lambda N, \lambda R_\alpha), \quad (6)$$

$$\lim_{\lambda \rightarrow \infty} \lambda^{-2} \rho_0(\lambda^{-1/3} r) = \lim_{\lambda \rightarrow \infty} \lambda^{-2} \rho(\lambda^{-1/3} r). \quad (7)$$

Since, on the length scale $\lambda^{-1/3}r$ both the core and valence regions vanish in the $\lambda \rightarrow \infty$ limit,⁷ it is clear that TF theory is a theory of the *bulk* electrons. This provides an informal understanding of the incorrect behavior of TF theory near in and far out, and also for the absence of molecular binding, which is a property of the valence region.

In TFD λ W theory, the presence of the gradient term corrects the qualitative near and far behavior of the density, with a cusp condition on the spherically averaged ρ_s near the nucleus,

$$\left. \frac{\partial \rho_s}{\partial r} \right|_{r=0} = -\frac{Z}{\lambda} \rho(0), \quad (8)$$

and an exponential decay into the vacuum,¹¹

$$\rho \sim r^{-2} \exp[-8\mu/\lambda]^{1/2} r. \quad (9)$$

We note that the Weizsäcker and Dirac corrections to the energy are $\sim O(Z^2)$ and $\sim O(Z^{4/3})$, respectively, and consequently do not affect the limits (6), (7).

Although real atomic densities do not have visible quantum fluctuations, they have a piecewise exponential structure,²² and radial atomic densities show pronounced shell structure, corresponding to regions of different exponential decay. None of the Thomas–Fermi-type theories produce such a shell structure. The origin of the shell structure has been traced both to the N -derivative discontinuities of the kinetic functional²³ and the derivative discontinuity in k space of the dielectric response function.^{3,12} Since the theories studied here are continuously differentiable, we do not expect the correct reproduction of a shell structure by any functional of the Thomas–Fermi type.

We now briefly survey some important numerical results in the literature. Atomic energies using Thomas–Fermi-type models have been computed by many workers^{5,8,24} (see Yang⁸ for some recent calculations). Also, the optimal choice of λ in the TFD λ W model for the reproduction of atomic energies, has been studied.^{8,24} von Weizsäcker proposed $\lambda=1$, although it was later demonstrated¹⁷ that in the slowly varying uniform electron gas, $\lambda=\frac{1}{9}$. Further studies by many authors^{5,8,19} have demonstrated that an empirical value of $\frac{1}{5}$ is near-optimal for reproducing atomic energies. However, it is as yet unclear what value of λ is best for the reproduction of molecular properties, such as binding energies and geometries.

In molecules, few calculations exist. As mentioned, from the nonbinding theorem of Teller¹⁵ (which was extended and improved by Balazs¹⁶ and Lieb and Simon⁷), Thomas–Fermi-type models without gradient corrections are unstable with respect to dissociation. In some early calculations, where several approximations (including a constrained density) were made in solving the Euler equation (1), Yonei⁶ concluded that TFD λ W, with $\lambda=\frac{1}{5}$, gave good qualitative dissociation curves for the N_2 molecule. However, Gross and Dreizler,¹¹ who solved the Euler equation in true variational TFD λ W calculations, could not find any evidence of binding at this λ value. Berk⁹ demonstrated that the Yonei calculations violated a lower bound result for the energy, and thus could not be considered reliable. Consequently, the problem of binding is still unresolved.

Finally, we remark on the problem of the size-consistency problem of molecular binding. For a separated molecule to minimize at infinite separation to the sum of atomic energies, all atoms must minimize with the same μ , otherwise there will be a flow of charge between the systems to balance the chemical potentials. It is then clear that TF

theory is exactly size consistent. This will not be the case for TFD λ W theory (or TFD theory), although the variation in μ among atoms, and the consequent violation of size consistency, will be λ dependent. We return to this point later.

III. SOLUTION OF THE EULER EQUATION

To perform definitive numerical calculations using Thomas–Fermi-type theories, we require a method to solve the Euler equation (1). We have adopted the Gaussian basis-set expansion approach of quantum chemistry, and have constructed a general purpose code FERMION for polyatomic molecules.

A. Evaluation of the Lagrangian in a Gaussian basis

Minimization of the Lagrangian $L = E - \mu N$ is subject to the constraint of positivity of ρ (as is usual, the further N representability constraint $\int |\nabla \rho^{1/2}|^2 d\mathbf{r} < \infty$ is automatically satisfied in our finite basis set expansion). We explicitly force positivity via

$$\rho = \phi^2. \quad (10)$$

Then ϕ is expanded in a Gaussian basis set η_i ,

$$\phi = \sum_i c_i \eta_i. \quad (11)$$

Around each nuclear center A , these are Cartesian Gaussians,

$$\eta = (x - x_A)^i (y - y_A)^j (z - z_A)^k e^{-\alpha(r - r_A)^2}. \quad (12)$$

We have also implemented contracted Gaussians, where each basis function η_i is itself a contraction of the form (11).

The evaluation of the Lagrangian requires several integrals, which are well known from implementing Kohn–Sham theory. The nuclear attraction and Coulomb integrals are Gaussian integrals that can be evaluated analytically. The kinetic and exchange–correlation functionals are of the form

$$F[\rho] = \int f(\rho, |\nabla \rho|) d\mathbf{r}. \quad (13)$$

These may be integrated using standard numerical quadrature schemes. We use the Becke atomic partitioning,²⁵ Euler–Maclaurin radial quadrature,²⁶ and Lebedev or Legendre angular quadrature.^{26,27} It should be noted that since the grid integral is an order of magnitude larger than usually encountered in Kohn–Sham theory, a very large quadrature is needed to yield sufficient accuracy for energy optimization.

B. Optimization

Due to the highly nonquadratic nature of the kinetic energy, the optimization of L with respect to c_i is a nontrivial problem. The iterative self-consistent procedure commonly used in Kohn–Sham calculations does not work, and we require more robust minimization techniques. Moreover, the Hessian matrix has a large spread of eigenvalues. Consequently, first derivative methods such as conjugate gradient minimization and quasi-Newton search²⁸ perform poorly, requiring many hundreds of iterations to achieve convergence. It is not yet clear how to precondition these methods for our problem. Also, we mention that these problems are exacerbated

if we incorporate the constraint $\int \rho d\mathbf{r} = N$ directly into an energy minimization, rather than via the Euler equation (1).

We have found that an efficient optimizer is provided by the second-derivative Newton–Raphson search.²⁸ We note that such a scheme has also been used by Yang⁸ in studies of atoms. Here the gradient vector \mathbf{d} is taken as

$$d_i = \sum_j H_{ij}^{-1} g_j, \quad (14)$$

where $H_{ij} = \partial^2 L / \partial c_i \partial c_j$ and $g_j = \partial L / \partial c_j$. At the solution point $\partial L / \partial c_j = 0$, this may be written as a Brillouin condition,

$$\left\langle \eta_i \left| \frac{\delta T_s}{\delta \rho} + v_x + v_J + v_{\text{ext}} - \mu \right| \phi \right\rangle = 0, \quad \forall i, \quad (15)$$

where $v_x = \delta E_x / \delta \rho$ and $v_J = \int \rho(\mathbf{r}_2) r_{12}^{-1} d\mathbf{r}_2$.

We note that the derivatives of L are simple to evaluate using the methods described in the previous section. Starting from a given orbital (initially chosen at random) and given μ , we perform a one-dimensional minimization of the Lagrangian with respect to λ , along $\phi + \lambda \sum_i d_i \eta_i$, and iterate this procedure to convergence. Typically less than ten iterations are required for convergence in L to an absolute tolerance of 10^{-5} Hartrees.

Since the Euler equation is nonlinear, convergence from a random starting point to the global minimum is not assured. Consequently, it is necessary to perform multiple minimizations from different starting points. For the calculations in this work, it appears that the global minimum can be located within five to ten independent minimizations.

To complete the solution of the Euler equation we now need to solve for μ such that $\int \rho d\mathbf{r} = N$. This is a one-dimensional root search that we perform by bisection. At each bisection step, we re-minimize our Lagrangian for the new bounding values of μ . Typically only a few bisection steps are required to achieve our target tolerance of 10^{-5} on the normalization integral.

C. Nuclear derivatives

The evaluation of nuclear derivatives is trivial due to the simple structure of the Euler equation. Let us consider some nuclear coordinate R . Then the energy derivative is given by

$$\frac{dE}{dR} = \frac{\partial E}{\partial R} + \frac{\partial E}{\partial c} \frac{\partial c}{\partial R}. \quad (16)$$

Through the usual route of relating $\partial E / \partial c$ to $\partial N / \partial c$ through the Euler equation, under the constraint $dN/dR = 0$, we may transform (16) to

$$\frac{dE}{dR} = \frac{\partial E}{\partial R} - \mu \frac{\partial N}{\partial R}. \quad (17)$$

The corresponding partial derivatives are straightforward to evaluate.

We have implemented a geometry optimizer that uses the Cartesian nuclear derivatives in a quasi-Newton (Broyden–Fletcher–Goldfarb–Shanno) minimization²⁸ of the energy.

TABLE I. Atomic energies using various Thomas–Fermi-type models, compared with literature and Hartree–Fock results. The literature results for Ne are taken from TF (exact formula), TFD, TFDW [Tomishima and Yonei (Ref. 5)], TFD λ W [Yang (Ref. 8)], and the HF values from Clementi and Roetti (Ref. 29).

	TF	TFD	TFD $\frac{1}{9}$ W	TFD $\frac{1}{5}$ W	TFDW	HF
H	−0.7491	−1.0224	−0.6664	−0.5666	−0.2618	−0.5000
He	−3.8234	−4.6093	−3.2228	−2.8184	−1.4775	−2.8617
Li	−9.8414	−11.3465	−8.2515	−7.3227	−4.1054	−7.4327
Be	−19.2464	−21.6413	−16.1631	−14.4841	−8.4922	−14.5730
B	−32.3865	−35.8191	−27.2876	−24.6284	−14.9258	−24.5291
C	−49.5281	−54.1558	−41.9052	−38.0332	−23.6568	−37.6886
N	−70.9520	−76.8929	−60.2622	−54.9428	−34.9084	−54.4009
O	−96.8564	−104.2472	−82.5798	−75.5765	−48.8831	−74.8094
F	−127.4524	−136.4158	−109.0592	−100.1345	−65.7674	−99.4094
Ne	−162.9263	−173.5801	−139.8865	−128.8014	−85.7343	−128.5471
Ne (lit)	−165.61	−176.3	−139.91	−128.83	−86.43	

IV. BENCHMARK CALCULATIONS

We now describe our calculations on a variety of atomic and diatomic systems.

A. Atoms

1. Total energies

Our goal in this section is to present benchmark calculations on atoms. Here we present the total energies for the neutral atoms H through Ne.

Preliminary investigations indicate that all first-row atoms minimize with spherical densities; consequently we constrain our atoms to be spherical. We use a large grid with 1000 radial points between 0 and 25 Bohr (no angular integration is required due to spherical symmetry). The basis set consists of s -type Gaussians of the form $\exp(-m^n r^2)$, for integer n . Our tabulated calculations use $m=3$ and $n=-4\cdots 14$, a total of 19 basis functions with exponents from $10^{-2}\cdots 10^7$. All energy optimizations are converged to 10^{-5} Hartrees.

Listed in Table I are the total energies for all our systems, for (Ref. 29) TFD λ W with $\lambda=\frac{1}{9}, \frac{1}{5}, 1$, and also for TF and TFD theory. Literature results for the neon atom are also given as Ne(lit); the TF energy is from the exact formula (5), the TFD and TFDW energies are from Tomishima and Yonei, and the TFD λ W energies are from Yang.¹⁸ Exact Hartree–Fock (HF) energies from Clementi and Roetti²⁹ are included for a comparison.

How accurate are our results? From comparing our neon TF energy with that from the Milne formula, it is true that our basis set is incomplete in that case. However, as discussed in Sec. II, the true TF (and TFD) densities are singular at the nucleus, and this contributes a significant proportion of the core energy. We cannot expect to capture such behavior using any basis-set procedure that does not explicitly include the divergence.

A better test is to examine the TFD λ W energies. We see that for the neon atom, our results lie above those of Yang, and Tomishima and Yonei. However, the method used by Yang (the finite difference solution of the Euler equation) is not strictly variational. We can estimate the basis limit in our approach by extrapolating the basis set. In the limit $m\rightarrow 1$ and the range of $m^n\rightarrow[-\infty, \infty]$, we have a complete basis

set. The energy is very insensitive to changing the lower bound of m^n , consequently in Fig. 1, we have extrapolated the neon TFD $\frac{1}{9}$ W energy as a function of m and the upper bound m^n . We see that our calculations are converged to an accuracy of better than 1 milliHartree. Similar convergence is observed for the other TFD λ W models.

Comparing our TFD λ W energies with the Hartree–Fock energies, we confirm the established result, that TFD $\frac{1}{5}$ W theory best reproduces atomic energies.

It is also of some interest to examine the chemical potential μ . As mentioned earlier, Thomas–Fermi theory yields exactly $\mu=0$. In Table II, we present the chemical potentials for the atoms using our various models. The chemical potential is very sensitive to the size of the basis set, thus our results are probably not accurate beyond the first significant figure. We observe very small μ for our TF calculations, in accordance with the theoretical considerations in Sec. II. In TFD and TFD λ W models, the chemical potential does take

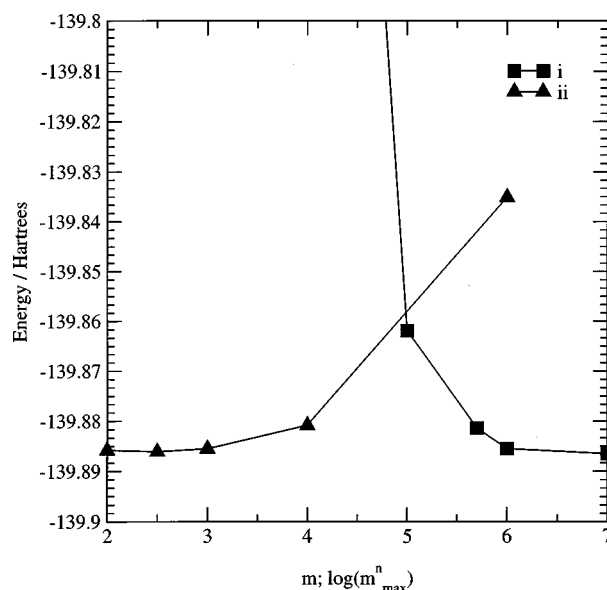


FIG. 1. Convergence of the neon energy TFD $\frac{1}{9}$ W energy using various basis sets. (i) Changing m^n_{\max} , for $m=3$. (ii) Changing m , with exponents $m^{-4}\cdots m^{14}$.

TABLE II. Atomic chemical potentials using various Thomas–Fermi-type models.

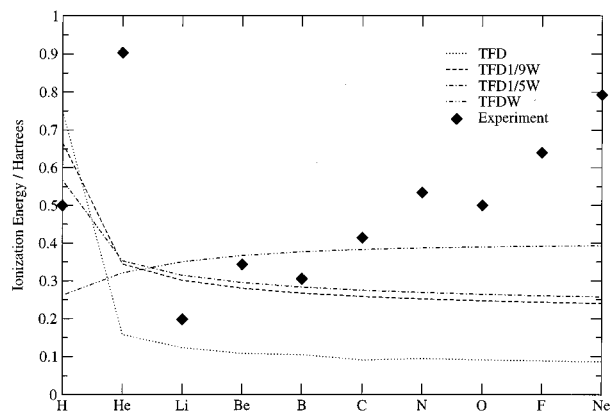
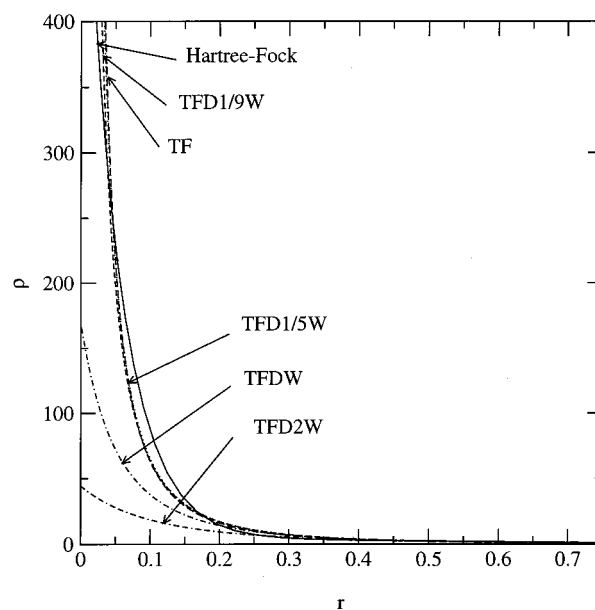
	TF	TFD	TFD $\frac{1}{9}W$	TFD $\frac{1}{5}W$	TFDW
H	0.001	−0.049	−0.059	−0.066	−0.071
He	0.002	−0.051	−0.062	−0.070	−0.108
Li	0.003	−0.051	−0.063	−0.072	−0.131
Be	0.003	−0.050	−0.063	−0.074	−0.145
B	0.002	−0.049	−0.063	−0.074	−0.156
C	0.003	−0.048	−0.064	−0.075	−0.163
N	0.003	−0.048	−0.064	−0.076	−0.169
O	0.003	−0.047	−0.064	−0.076	−0.174
F	0.003	−0.047	−0.064	−0.076	−0.178
Ne	0.003	−0.046	−0.064	−0.077	−0.181

small nonzero values that increase (in magnitude) monotonically with λ . This indicates that the system wishes to minimize with an electron number other than $N=Z$. Still, in absolute terms, the chemical potential is very small and very similar between the atoms, indicating that both charge neutrality and size consistency are approximately maintained by all our Thomas–Fermi-type models.

In Fig. 2 we plot the ionization energies using the TFD λ W models. We see that they are monotonic curves whose gradient is determined by λ (the gradient increases with increasing λ). It is not surprising that we do not reproduce the nonmonotonic nature of the true ionization potential, as the origin of the variation between atoms lies in the fermionic nature of the electrons, and the consequent occupation of different orbitals with different angular momenta. However, due to the different spin states of the atoms, it may be possible to account for some of these effects through a spin-density functional treatment. Nonetheless, the true ionization energies of the atoms¹⁷ do fluctuate around the mean ionization energies given by our models.

2. Densities

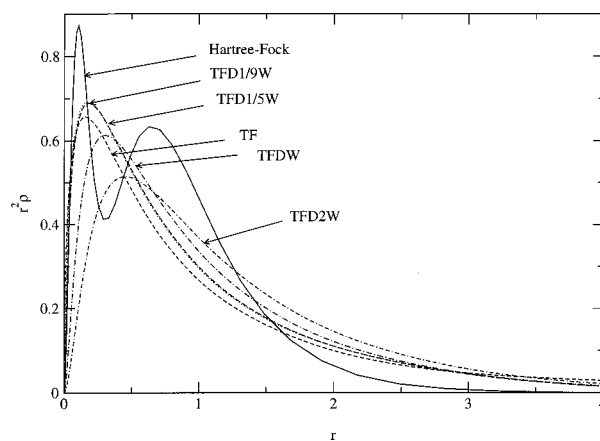
Here we examine the densities of our Thomas–Fermi-type models. In Figs. 3 and 4 we plot the density and radial density given by a variety of Thomas–Fermi-type models as compared with the Hartree–Fock densities, for the neon atom. As expected, no shell structure is observed, the

FIG. 2. Ionization energies of first-row atoms with TFD λ W models.FIG. 3. Density ρ with various Thomas–Fermi-type models.

Thomas–Fermi densities displaying an averaging over the shell structure of the Hartree–Fock density (computed at the TZ2P level³⁰ with CADPAC).³¹ The divergence of the Thomas–Fermi density is clearly seen. We further note that despite the *formal* improvement offered by the inclusion of the Weizsäcker term, in practice, the TFD λ W density is not very different from the Thomas–Fermi density, being very strongly peaked at the nucleus, and decaying in a similar fashion over the chemically relevant regions of the atom. We see the progressive effect of increasing λ is to lower the value of the density at the nucleus, and to relax the density so the peak in the radial density flattens and moves outward into the valence region.

B. Diatomic molecules

Our goal in this section is to present benchmark calculations on diatomics to address the problem of binding in TFD λ W theory.

FIG. 4. Radial density $r^2\rho$ with various Thomas–Fermi-type models.

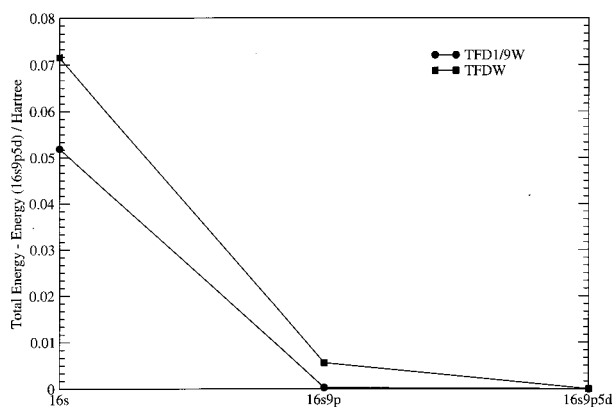


FIG. 5. Convergence of the N_2 energy at 2 Bohr with angular momentum functions. Plotted is the energy with various basis sets ($16s, 16s9p, 16s9p5d$)—energy ($16s9p5d$), for $TFD_{\frac{1}{9}}W$ and $TFDW$ theory.

We perform calculations in cylindrical symmetry, using a large basis set of s -, p -, and d -type Gaussians (our program does not support higher angular momentum functions). Due to the symmetry constraints we choose only the p_x and d_{x^2} functions, where x is the molecular axis. The exponents are chosen as a series m^n as in the atomic calculations; for s Gaussians, we take $m=3$ and $n=-2 \cdots 12$, for p Gaussians we take $m=3$ and $n=-6 \cdots 2$, and for d Gaussians we take $m=3$ and $n=-6 \cdots -2$. This is a $16s9p5d$ basis on each atom, which gives a total of 60 basis functions for the diatomic molecule. Our quadrature is chosen as a large two dimensional Legendre quadrature, with roughly 2000 points.

We have performed a number of basis-set convergence studies, to assess the quality of our calculations. Our basis sets are most accurate for calculations with $TFD_{\frac{1}{9}}W$ theory, but even in our worst case, the s , p , and d basis sets are well saturated and residual basis set effects with respect to these angular momentum functions are estimated to be of the order of 1 milliHartree. With respect to contributions from higher angular momentum functions, we estimate that our $16s9p5d$ calculations with $TFD_{\frac{1}{9}}W$ and $TFD_{\frac{1}{5}}W$ theory are within ~ 1 milliHartree of the basis set limit, and calculations with $TFDW$ and $TFD2W$ are within ~ 10 milliHartrees of the basis set limit. We see little reason to pursue these calculations to higher accuracy. In Fig. 5, we plot the convergence of the energy with respect to angular momentum for the N_2 molecule at 2 Bohr.

In Fig. 6 we present the binding curve for the N_2 molecule with $TFD_{\frac{1}{5}}W$ theory. We include for comparison the literature results of Yonei,⁶ Gross and Dreizler,¹¹ and Berk.⁹ We see that our results (which are variational upper bounds) lie below the upper bound of Gross and Dreizler, and above the lower bound of Berk. We see that the Yonei calculation does not obey these bounds.

We now discuss various qualitative features of molecular binding in the $TFD_{\lambda}W$ model. Examining the N_2 binding curves in Fig. 7, we see that the strength of binding increases as λ increases, and the total energy increases (becomes more positive). These results are simple to understand. As we saw in Fig. 4, increasing λ pushes more electrons into the valence

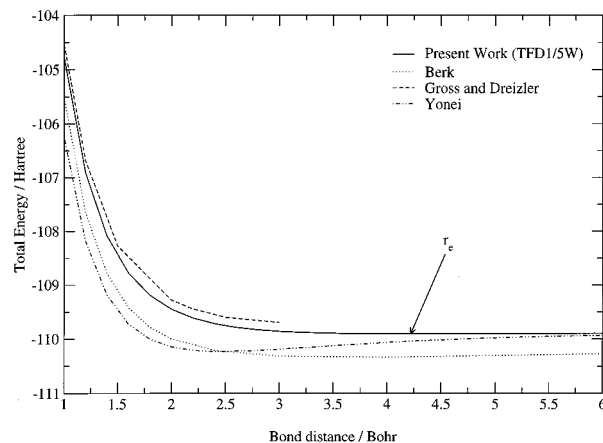


FIG. 6. Binding curve of N_2 using $TFD_{\frac{1}{5}}W$ theory, with the present work, as compared to literature results.

region, which should increase the strength of binding (for example, from Hellmann–Feynman arguments). The overall increase in energy is simply from the increased magnitude in the kinetic energy (which is positive). A simple optimization of λ to reproduce the experimental bond distance yields $\lambda \sim 2$. As $\lambda \rightarrow \infty$, however, the kinetic energy completely swamps the nuclear contribution, and we do not expect binding in the limit $\lambda/Z \rightarrow \infty$.

Although the bond distance of N_2 is well reproduced at $\lambda=2$, the molecule is highly overbound, when compared with Hartree–Fock theory. In contrast, total energies are best reproduced with $\lambda=\frac{1}{5}$, although the binding energy is far too small. This inability to reproduce both the total energy and binding energy by optimizing λ reflects the different energy contributions of the core, bulk, and valence regions, whose distribution cannot be satisfactorily modeled by a single parameter.

In Table III, we present binding energies and geometries for a range of diatomics, with various $TFD_{\lambda}W$ models, and Hartree–Fock (unrestricted TZ2P) calculations for comparison. Our geometries have been optimized to 0.01 Bohr; however, due to the extreme flatness of the $TFD_{\frac{1}{9}}W$ and $TFD_{\frac{1}{5}}W$ binding curves, our equilibrium geometries for these models

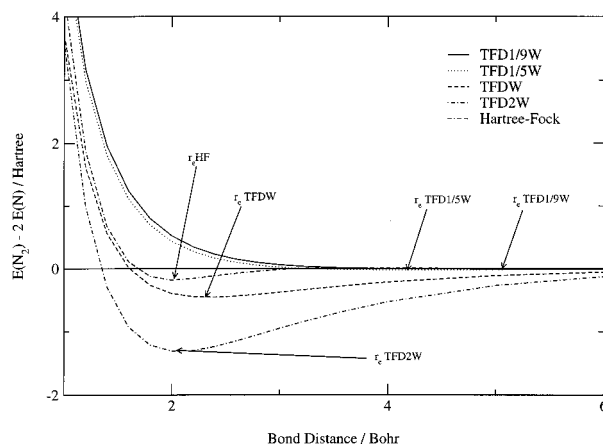


FIG. 7. Binding curve of N_2 using $TFD_{\lambda}W$ theories, as compared with unrestricted Hartree–Fock (TZ2P).

TABLE III. Binding energies $\Delta E = E(A) + E(B) - E(AB)$ in Hartrees and optimized bond lengths in Bohr, using TFD λ W theories, and Hartree–Fock (unrestricted TZ2P) theory. Negative binding energies indicate local minima.

	TFD $\frac{1}{9}$ W		TFD $\frac{1}{5}$ W		TFDW		TFD2W		HF	
	ΔE	r_e	ΔE	r_e	ΔE	r_e	ΔE	r_e	ΔE	r_e
H ₂	0.006	3.41	0.012	3.00	0.051	3.27	0.048	4.79	0.135	1.38
N ₂	0.008	4.94	0.022	4.24	0.463	2.35	1.349	2.08	0.182	2.02
O ₂	0.008	5.04	0.022	4.34	0.500	2.36	1.584	2.02	0.054	2.19
F ₂	0.008	5.14	0.023	4.42	0.532	2.38	1.807	1.98	−0.055	2.52
HF	0.006	4.27	0.016	3.72	0.147	2.82	0.265	2.96	0.155	1.70
CO	0.008	4.94	0.022	4.24	0.458	2.34	1.318	2.09	0.277	2.09

may be accurate only to two significant figures (although the binding energies will be accurate to within the errors described above). The bond distances and binding energies are monotonic functions of the number of electrons (the binding energies increase monotonically with N). We see that increasing λ increases the bond energy and shortens the bond distance in the diatomics (except for H₂, due to the high λ/Z ratio, as discussed earlier). It would appear that molecules are bound even with $\lambda = \frac{1}{9}$, although with binding energies of only a few milliHartrees. Consequently, we feel it is accurate to conclude that binding is described by the TFD λ W model, and is correct qualitatively insofar as the bond distances are the correct order of magnitude. Moreover, with $\lambda = \frac{1}{5}$ and $\lambda = \frac{1}{9}$, we obtain the same trend in the bond distances as in Hartree–Fock theory. However, this is a long way from an acceptable chemical accuracy. The correct N -dependent variation in binding energies, stemming from the stepwise occupation of σ - and π -type orbitals, and corresponding shell structure in the atoms, is not produced, and indeed such a feature is a challenge to reproduce using a Thomas–Fermi-type functional. We note that all the diatomic systems studied (with the exception of O₂) are closed shell systems, and thus we do not expect our results to improve with a spin-dependent formulation.

We finally comment on the size-consistency problem, as mentioned in Sec. II. In homonuclear diatomics, there is, of course, no size-consistency problem, as the infinitely separated atoms have the same μ . We have carried out preliminary investigations on HF at infinite separation. These indicate that the flow of charge between atoms is small, but increases with increasing λ . With $\lambda = \frac{1}{9}$, the charge flow at infinity is ~ 0.001 with a negligible lowering of energy; with $\lambda = 1$, the charge flow is ~ 0.15 with the ionic state ~ 10 milliHartrees lower in energy than the neutral atoms. We note that these considerations do not affect the qualitative picture of binding in TFD λ W theory.

V. CONCLUSIONS

In this work, we have carried out a numerical study of the Thomas–Fermi–Dirac–von Weizsäcker energy model. Earlier studies have not been of sufficient accuracy to answer the important question as to whether this model includes molecular binding. To solve the Euler equation associated with this model, we have developed a general purpose Gaussian-based code, which can carry out energy and geom-

etry optimizations to high accuracy. We present benchmark calculations on atomic and diatomic systems. Our studies show that TFD λ W theory can offer a qualitative description of atomic and diatomic properties. For such a simple theory, it does very well, and indeed we can reproduce atomic total energies and molecular binding in a qualitative fashion. However, the more detailed description of atomic and molecular systems, which is a prerequisite for a chemically meaningful theory, is lacking. In particular, such properties that depend on the characteristics of separate electrons, such as their core/bulk/valence nature, or their angular momentum, are not described. As is well known, atomic shell structure is not reproduced, nor do we obtain a good optimized density, and the strength of molecular binding is generally a simple function of N .

We note that our studies have not included any description of spin, although this may be trivially treated through the spin-density analog of Thomas–Fermi theory, and the inclusion of spin will not affect our general conclusions above. The problems in TFD λ W theory are, of course, due to the approximate description of the kinetic energy and will not be fully resolved unless one returns to an explicit description of the electrons, which most likely requires a non-differentiable model such as in Kohn–Sham theory. However, it is still an open question as to how well one can do in some average manner with the optimum kinetic functional of the Thomas–Fermi type. We have tried to optimize the λ parameter in TFD λ W theory, but it offers only limited improvement. A detailed study should choose a more sophisticated framework of approximation, for example, a generalized gradient approximation,^{14,32,33}

$$T_s[\rho] = \int \rho^{5/3} f(\rho, |\nabla \rho|, \nabla^2 \rho) d\mathbf{r}, \quad (18)$$

or a nonlocal functional such as those studied in extended systems,^{12,13}

$$T_s[\rho] = \iint f[\rho(\mathbf{r}_1), \rho(\mathbf{r}_2)] g(k_F, r_{12}) d\mathbf{r}_1 d\mathbf{r}_2, \quad (19)$$

where k_F is the Fermi momentum. Once such a form has been decided, we may then apply the techniques from the optimization of exchange–correlation functionals to optimize the kinetic functional. The qualitatively correct features of the simple TFD λ W model offers some hope that a judicious

choice of fitting data may yield functionals that perform well over restricted classes of systems, and that can be used in an approximate description of matter.

- ¹L. H. Thomas, Proc. Cambridge Philos. Soc. **23**, 542 (1927).
- ²E. Fermi, Z. Phys. **48**, 73 (1928).
- ³P. Hohenberg and W. Kohn, Phys. Rev. B **136**, 864 (1964).
- ⁴W. Kohn and L. J. Sham, Phys. Rev. A **140**, 1133 (1965).
- ⁵Y. Tomishima and K. Yonei, J. Phys. Soc. Jpn. **21**, 142 (1966).
- ⁶K. Yonei, J. Phys. Soc. Jpn. **31**, 882 (1971).
- ⁷E. H. Lieb and B. Simon, Phys. Rev. Lett. **31**, 681 (1973).
- ⁸W. Yang, Phys. Rev. A **34**, 4575 (1986).
- ⁹A. Berk, Phys. Rev. A **28**, 1908 (1983).
- ¹⁰T. A. Wesolowski, Y. Ellinger, and J. Weber, J. Chem. Phys. **108**, 6078 (1998).
- ¹¹E. K. U. Gross and R. M. Dreizler, Phys. Rev. A **20**, 1798 (1979).
- ¹²L. W. Wang and M. P. Teter, Phys. Rev. B **45**, 13 196 (1992).
- ¹³M. Foley and P. A. Madden, Phys. Rev. B **53**, 10 589 (1996).
- ¹⁴G. K-L. Chan and N. C. Handy, J. Chem. Phys. **112**, 5639 (2000).
- ¹⁵E. Teller, Rev. Mod. Phys. **34**, 627 (1962).
- ¹⁶N. L. Balazs, Phys. Rev. **156**, 42 (1967).
- ¹⁷R. G. Parr and W. Yang, *Density Functional Theory of Atoms and Molecules* (Oxford University Press, Oxford, 1989).
- ¹⁸More specifically, Balazs has argued that binding is not possible if the density is a function of the total classical electrostatic potential.
- ¹⁹C. F. von Weizsäcker, Z. Phys. **96**, 431 (1935).
- ²⁰P. A. M. Dirac, Proc. Cambridge Philos. Soc. **26**, 376 (1930).
- ²¹E. H. Lieb, Rev. Mod. Phys. **53**, 603 (1981).
- ²²W.-P. Wang and R. G. Parr, Phys. Rev. A **16**, 891 (1977).
- ²³G. K-L. Chan and N. C. Handy, J. Chem. Phys. **59**, 2670 (1999).
- ²⁴W. Stieh, E. K. U. Gross, P. Malzacher, and R. M. Dreizler, Z. Phys. A **309**, 5 (1982).
- ²⁵A. D. Becke, J. Chem. Phys. **88**, 2547 (1988).
- ²⁶C. W. Murray, N. C. Handy, and G. J. Laming, Mol. Phys. **78**, 997 (1993).
- ²⁷V. I. Lebedev, Sibirsk. Mat. Zh **18**, 132 (1975); Russ. Acad. Sci. Dokl. Math. **45**, 593 (1992).
- ²⁸W. H. Press, S. A. Teukolsky, W. T. Vetterling, and B. P. Flannery, *Numerical Recipes in Fortran*, 2nd ed. (Cambridge University Press, Cambridge, 1992).
- ²⁹E. Clementi and E. Roetti, At. Data Nucl. Data Tables **14**, 177 (1974).
- ³⁰T. H. Dunning, Jr., J. Chem. Phys. **55**, 716 (1971). These basis sets are contracted $5s4p$ quality for the first-row atoms, and contracted $3s$ quality for H. In the TZ2P calculations, we have added polarization functions (p type for H, d type for other first-row atoms), with exponents 0.4, 0.1 for H, 1.2, 0.4 for C, 1.35, 0.45 for N, 1.35, 0.45 for O, 2.0, 0.67 for F.
- ³¹CADPAC: Cambridge Analytical Derivatives Package Issue 6.5, Cambridge, UK, 1998: A suite of quantum chemistry programs developed by R. D. Amos with contributions from I. L. Alberts, J. S. Andrews, S. M. Colwell, N. C. Handy, D. Jayatilaka, P. J. Knowles, R. Kobayashi, N. Koga, K. E. Laidig, P. E. Maslen, C. W. Murray, J. E. Rice, J. Sanz, E. D. Simandiras, A. J. Stone, M.-D. Su, and D. J. Tozer.
- ³²H. Lee, C. T. Lee, and R. G. Parr, Phys. Rev. A **44**, 768 (1991).
- ³³C. H. Hodges, Can. J. Phys. **51**, 1428 (1973).